DESIGN AND FABRICATION OF HIGH TEMPERATURE RESISTIVITY MEASUREMENT SETUP

Thesis Submitted for the Award of the Degree of

Master of Science

By

SUSHREE ROSYLA BARPANDA

Under the academic autonomy

National Institute of Technology, Rourkela

Under the Guidance of

Dr. Prakash Nath Vishwakarma
&
Dr. Dillip Kumar Pradhan

Department of Physics

National Institute of Technology

Rourkela-769008

DECLARATION

I hereby declare that the project work entitled “Design and Fabrication of high temperature resistivity measurement set-up” submitted to National Institute ofTechnology, Rourkela, is the record of an original work done by me under the guidance of Dr. Prakash NathVishwakarma and Dr. Dillip Ku. Pradhan, Assistant professor of NIT,Rourkela, and this project work has not performed the basis for the award of any degree or diploma/ associate-ship/fellowship and similar project if any.

Sushree Rosyla Barpanda

Roll- 409ph2081

NIT, Rourkela.

Department of Physics
National Institute of Technology
Rourkela – 769008 (Orissa)

CERTIFICATE

This is to certify that the thesis entitled "Design & Fabrication of High Temperature Resistivity Measurement Setup" submitted by Sushree Rosyla Barpanda in partial fulfilment of the requirements for the award of degree of Master of Science in Physics at National Institute of Technology, Rourkela is an authentic work carried out by her under our supervision. To the best of my knowledge, the work done in this thesis has not been submitted by any other university/ Institute for the award of any degree or diploma.

Dr. Prakash Nath Vishwakarma

Dr. Dillip Kumar Pradhan

ACKNOWLEDGEMENT

First and foremost, to my friend, pew mate and my collaborator, Kalyani Bhoi for working so hard for this project and for truly understanding my potential for this project.

I am heartily thankful to my supervisor, Dr. Dillip Kumar Pradhan and Dr. Prakash Nath Vishwakarma , whose encouragement, supervision and support from the preliminary to the concluding level enabled me to develop an understanding of the subject.

I cannot fully express my gratitude to the exceptional team at Department of Physics, NIT Rourkela including my friends. I am really thankful to Mr. Barun Ku. Barik, Mr. Achutya Ku. Biswal, Miss Jashashree Ray, Ph.D scholars, for their generosity, faith and superb guidance.

For the generous assistance in the research of this project, I would like to acknowledge the Central Workshop for extending their facilities for preparing my setup, Department of Chemistry for providing the required materials for my sample preparation and Department of Metallurgical and Material Science for the help in taking XRD.

I humbly prostrate myself before the Almighty for his grace and abundant blessings, which enabled me to complete this work successfully.

Last but not least I wish to avail myself of this opportunity, express a sense of gratitude and love to my beloved parents and my family for their manual support, strength, help and for everything.

Sushree Rosyla Barpanda

DEDICATED TO MY PARENTS

TABLE OF CONTENTS

LIST OF TABLES

LIST OF FIGURES

ABSTRACT

A high temperature resistivity measurement set-up has been designed consisting of a furnace and a four probe to measure the resistivity of prepared sample. The handmade furnace can withstand temperature up to 600^0C. The system also consists of an automatic temperature controller which uses the principle of an 'on-off' furnace controller. A K-type thermocouple is used to measure and control the furnace temperature and a Pt-100 sensor is used for sample temperature measurement. This Pt-100 sensor is connected with digital multimeter which gives its corresponding resistances for temperature conversion. The setup is connected with Kethley nanovolmeter and current source, which are interfaced with a computer using Lab-view software. This arrangement reduces the manual effort. In this experimental set up, both bulk and thin film samples can be investigated. We have prepared a ceramics oxide ($La_{2/3}Sr_{1/3}MnO_3$) by sol-gel auto combustion method and the formation of the compound has been checked using X-ray diffraction analysis. The crystal structure was found to be orthorhombic with lattice parameter a= 3.8550 A^0, b= 3.8367A^0 and c= 3.8794A^0. The temperature dependent resistivity of $La_{2/3}Sr_{1/3}MnO_3$ is presented as a test material to demonstrate the possibility and accuracy of the experimental set-up. The temperature dependent electrical resistivity follows Arrhenius behaviour.

CHAPTER-1

INTRODUCTION

The modern concept of electrical resistance was first discovered by G. S. Ohm, in 1926, who formulated the famous equation: V=IR, while working on direct-current circuit. The resistance is a function of temperature and stress for a given material. This property of resistance is employed in resistance-temperature conversion.

1.1 RESISTANCE AND IT'S ORIGIN:

The electrical resistance of an object is a measure of its opposition to the passage of an electric current. Electrical resistance of a circuit component or device is defined as the ratio of the voltage applied to the electric current which flows through it.

$$R = \frac{V}{I}$$

The SI unit of electrical resistance is the ohm (Ω). Resistance's reciprocal quantity is electrical conductance measured in siemens.

1.1.1 Causes of resistance:

In metals:

When an electrical potential difference (a voltage) is applied across the metal, the electrons drift from one end of the conductor to the other, under the influence of the electric field. Near room temperatures, the thermal motion of ions is the primary source of scattering of electrons (due to destructive interference of free electron waves on non-correlating potentials of ions), and is thus the prime cause of metal resistance. Imperfections of lattice also contribute into resistance,

although their contribution in pure metals is negligible. The longer the conductor, the more scattering events occur in each electron's path through the material, so the higher the resistance [1].

In semiconductor and insulator:

In semiconductors the position of the Fermi level is within the band gap, approximately half-way between the conduction band minimum and valence band maximum for intrinsic (undoped) semiconductors. This means that at zero kelvin, there are no free conduction electrons and the resistance is infinite. However, the resistance will continue to decrease as the charge carrier density in the conduction band increases. In extrinsic (doped) semiconductors, dopant atoms increase the majority charge carrier concentration by donating electrons to the conduction band or accepting holes in the valence band. For both types of donor or acceptor atoms, increasing the dopant density leads to a reduction in the resistance. Highly doped semiconductors hence behave like metallic. At very high temperatures, the contribution of thermally generated carriers will dominate over the contribution from dopant atoms and the resistance will decrease exponentially with temperature [1].

In superconductors:

When the electrical resistance of some material, drops to zero at its critical temperature then the material becomes superconductor. In a superconductor, below its critical temperature, there is no resistance because the scattering mechanisms are unable to impede the motion of the current carriers. As a negatively-charged electron moves through the space between two rows of positively-charged atoms, it interacts with another electron by exchanging an acoustic quanta called phonon. This distortion attracts a second electron to move in behind it. The two electrons form a weak attraction, travel together in a pair and encounter less resistance overall. The current is carried then by electrons moving in pairs called Cooper pairs. So they can carry large amounts of electrical current for long periods of time without losing energy as ohmic heat [2].

1.1.2 Temperature dependence of resistance:

Near room temperature, the electrical resistance of a typical metal increases linearly with increase in temperature, while the electrical resistance of a typical semiconductor decreases with rising temperature. To the first order, the temperature dependence of resistance follows the relation

$$R = R_o + [\alpha(T - T_o) + 1]$$

where, T is its temperature, T_0 is a reference temperature (usually zero Kelvin or room temperature), R_0 is the resistance at T_0, and α is the coefficient of change in resistivity per unit temperature also known as, temperature coefficient of resistance. The constant α depends only on the material being considered.

Intrinsic semiconductors become better conductors as the temperature increases; the electrons are jumped to the conduction energy band by thermal energy, where they flow freely and in doing so leave behind holes in the valence band which also flow freely. The electric resistance of a typical intrinsic (non-doped) semiconductor decreases exponentially with rise temperature:

$$R = R_o e^{-\alpha T}$$

Extrinsic (doped) semiconductors have a far more complicated temperature profile. As temperature increases starting from absolute zero, they first decrease steeply in resistance as the carriers leave the donors or acceptors. At higher temperatures it will behave like intrinsic semiconductors as the carriers from the donors/acceptors become insignificant compared to the thermally generated carriers[1].

1.2 RESISTIVITY

The quantitative measure of a material's opposition to the flow of current is called resistivity. It depends only on the composition of the material and not on the shape and size.

$$R = \frac{\rho L}{A}$$

where:R is the resistance(ohms), ρ is resistivity(ohm-meters), L is the length(meters), and A is the cross-sectional area(square-meters).

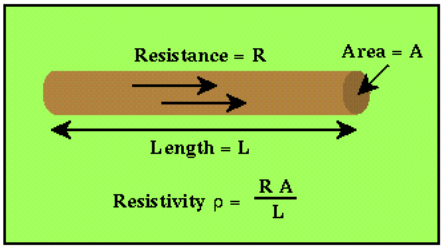

Fig 1.1: Resistivity of a material [3]

Although the resistivity is temperature dependent, it can be used to calculate the resistance of a wire of given geometry at a given temperature.

The resistivity of the material changes with temperature. For many materials, the change is a simple linear function of temperature: $\rho(T) = \rho_0[1-\alpha(T-T_0)]$, where: ρ(T) = resistivity at temperature T, ρ_0 =resistivity at temperature T_0, α =temperature coefficient of resistivity [4].

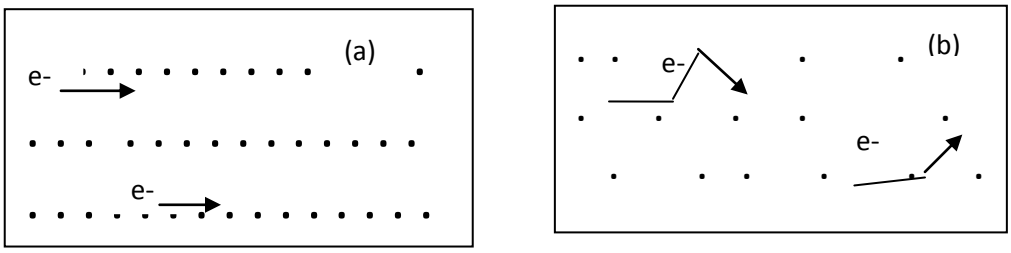

Fig 1.2: movement of electron in (a) cold body (b) hot body. In cold body, the ions are more ordered and the electrons move without much scattering. In hot body, due to vibration of ions, the electrons undergo more scattering.

Materials	**Resistivity, ρ(ohm-meter)**
Metals	10^{-8}
Semiconductors	Variable
Electrolytes	Variable
Insulators	10^{16}
Superconductors	0(exactly)

Table 1.1: Resistivity of various materials [1].

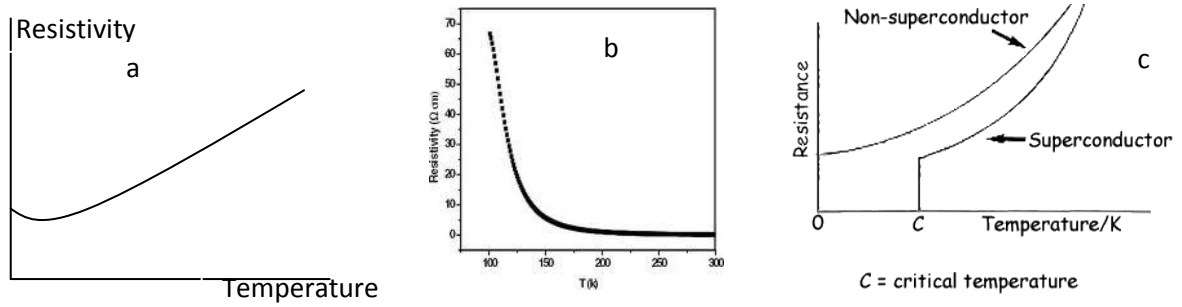

Fig 1.3: Resistivity vs. temperature plot for a) metal b) semiconductor c) superconductor

Table 1.1 shows the resistivity of the various materials. The temperature dependent of resistivity of the various materials as shown in Figure 1.3.

1.3 RESISTIVITY MEASUREMENT METHODS

The resistivity is determined by measuring resistance R and the dimensions of the sample (length l, width/ thickness d). The resistance R is usually determined by a voltage-current method. A current of known I value is fed into the sample and the voltage V is measured via point contact. From these measurements the resistivity is calculated as,

$$\rho = R\frac{w \times d}{l}$$

There are various methods of resistivity measurements:

1.3.1 Two probe method:

The test specimen for the two probe method may be in the form of strip, rod or bar. The two probe method always gives a value with contributions from contact wires, contact resistance and hence not advisable in case of metals where the sample resistance is very low.

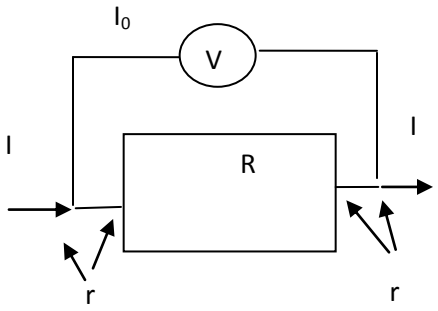

Fig 1.4: schematic diagram of two probe.

Since the internal resistance of voltmeter is very high (10^6 Ω), hence I_0<<I,so that I-I_0~I. so the voltage measured by the voltmeter will be,

$$=(I-I_0)(r+R+r).$$

So, r+R+r gives an error to the measurement. However this method can be applied (if R>>2r) for highly resistive samples.

1.3.2 Four probe method:

The advantage of four probe method is that it minimizes the other contributions (lead resistance, contact resistance, etc.) to the resistance measurement which results an accurate measurement of sample resistance. This includes four equally spaced probes in contact with a material of unknown resistance. The outer two probes are used for sourcing the current and the two inner probes are used for measuring the resulting voltage drop across the surface of the sample.

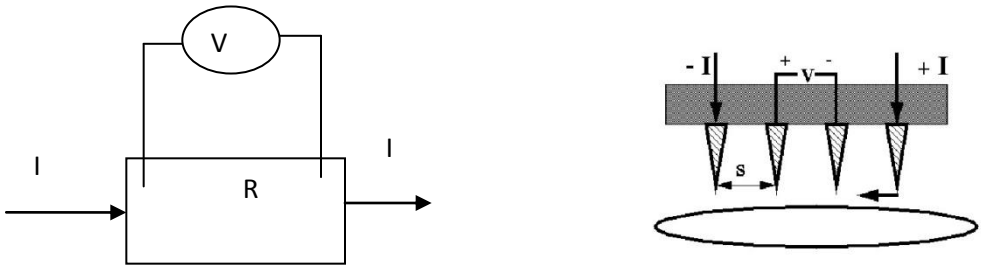

Fig 1.5: schematic diagram of four probe.

Here according to the diagram, the voltage measured by the voltmeter is =(I-I_0)R. Hence, the sample voltage measured is more accurate in four probe.

1.3.3 Van der Pauw method:

This technique is commonly used for measuring sheet resistance of a material. For samples of irregular shape and size, the two and four probe method is not applicable and so choice is Van der Pauw method. This method includes the measurement of two resistance, R_A and R_B as shown in Figure given below.

$R_A=V_{43}/I_{12}$

$R_B=V_{14}/I_{23}$

The sheet resistance is related to these calculated resistance by the van der pauw formula,

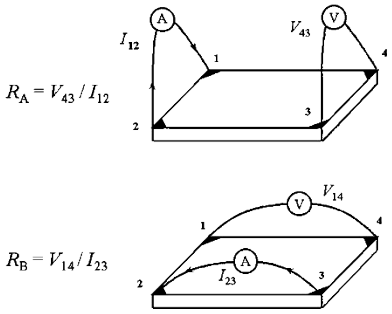

Fig 1.6 : Van-der Pauw measurement in different configurations

$$e^{\frac{-\pi R_A}{R_s}} + e^{\frac{-\pi R_B}{R_s}} = 1$$

where, R_s is sheet resistance to be determined. If R_A and R_B are similar, then resistivity is given by

$$\rho = \frac{\pi d}{\ln 2}\frac{(R_A + R_B)}{2}$$

where, d is the thickness of the sample. If R_A and R_B are not similar then resistivity modifies as,

$$\rho = \frac{\pi d}{\ln 2}\frac{(R_A + R_B)}{2} f\left(\frac{R_A}{R_B}\right)$$

Where $f\left(\frac{R_A}{R_B}\right)$ is the function of the ratio $\frac{R_A}{R_B}$ only.

1.4 RESISTANCE TEMPERATURE DETECTOR (RTDs)

Resistance Temperature Detectors (RTDs), as the name implies, are sensors used to measure temperature by correlating the resistance of the RTD element with temperature. Most RTD elements consist of a length of fine coiled wire wrapped around a ceramic or glass core. The element is usually quite fragile, so it is often placed inside a sheathed probe to protect it. The RTD element is made from a pure material whose resistance at various temperatures has been documented. The material has a predictable change in resistance as the temperature changes; the predictable change is used to determine temperature. Some frequently used RTDs are: (i) Platinum (most popular and accurate), (ii) Nickel, (iii) Copper, (iv) Balco (rare), (v) Tungsten (rare), etc [5].

1.4.1 Benefit of using a RTD :

The RTD is one of the most accurate temperature sensors. It not only provides good accuracy, but also provides excellent stability and repeatability. RTDs are relatively immune to electrical noise and therefore well suited for temperature measurement in industrial environments, especially around motors, generators and other high voltage equipment [5].

METAL	**RESISTIVITY ohm/cmf** **Cmf = circular mil foot**
Gold (Au)	13
Silver (Ag)	8.8
Copper (Cu)	9.26
Platinum (Pt)	59
Tungsten (W)	30
Nickel (Ni)	36

Table 1.2 : Resistivities of common RTD materials [6]

Because of their lower resistivity, gold and silver are rarely used as RTD elements. Tungsten is reserved for very high temperature applications because of relatively high resistivity. The most common RTD's are made of either platinum, nickel, or nickel alloys. The economical nickel derivative wires are used over a limited temperature range. They are quite non-linear and tend to drift with time. For measurement integrity, platinum is the obvious choice [6]

1.4.2 Platinum resistance thermometer(PRTs):

Platinum Resistance thermometers are temperature sensors that exploit the predictable change in electrical resistance of platinum with changing temperature. These are being used in place of thermocouples in industrial applications at temperatures below 600 ^{0}C. At higher temperatures, it becomes difficult to prevent the platinum from being contaminated by impurities from the metal sheath of the thermometer. Platinum resistance thermometer requires a small current to pass through it, to determine its resistance at different temperatures. Platinum has a linear resistance-temperature relationship; we can use this method to find the resistance at different temperatures.

Platinum Resistance thermometer consists of a fine platinum wire (platinum coil) wound in a non-inductive way on a mica frame M (Figure 1.7). The ends of this wire are soldered to points A and C from which two thick leads run along the length of the glass tube (that encloses the set up) and are connected to two terminals (P, P) fixed on the cap of the tube. These are the platinum wire leads**.** Also, by the side of these leads, another set of leads run parallel and are connected to the terminals (C, C) fixed on the cap of the tube. These are called compensating leads and are joined together inside the glass tube. The compensating leads and the platinum wire are separated from each other by mica or porcelain separators (D, D). The electrical resistance of the (P, P) leads is same as that of the (C, C) leads [7].

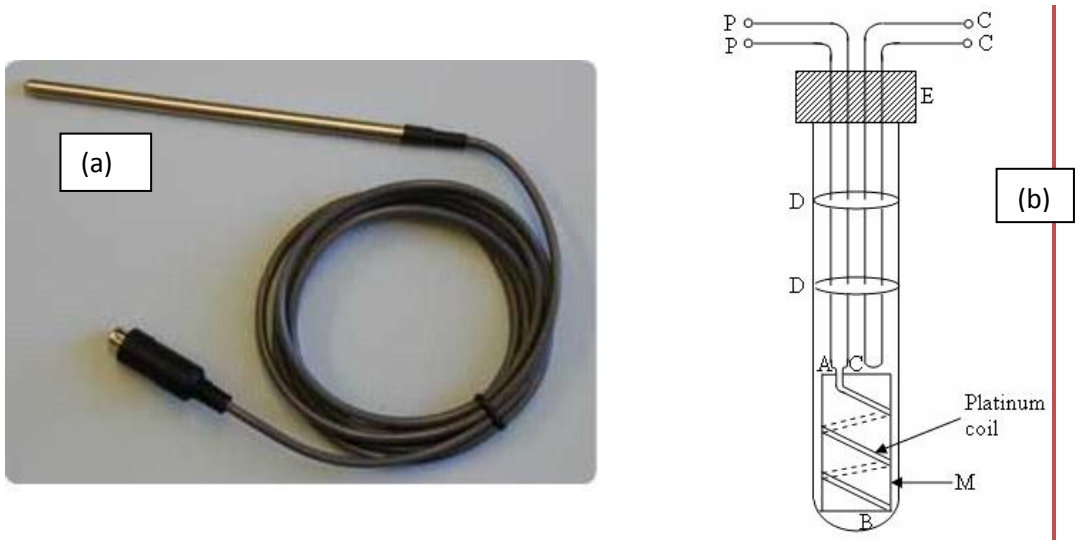

Fig 1.7 : Platinum resistance thermometer (a) Pt-100 probe (b) its schematic representation.[7]

The most common type (PT100) has a resistance of 100 ohms at 0 °C and 138.4 ohms at 100 °C. There are also PT1000 sensors that have a resistance of 1000 ohms at 0 °C. The linearization equation of its temperature dependence is:

$$R_t = R_0 * (1 + A* t + B*t^2 + C*(t-100)* t^3)$$

where, R_t is the resistance at temperature t, R_0 is the resistance at 0 °C, A= 3.9083x10^{-3}, B = -5.775 x$10^{-7,}$ C = -4.183 x10^{-12} (below 0 °C), or C = 0 (above 0 °C).

For a PT100 sensor, a 1 °C temperature change will cause a 0.384 ohm change in resistance, so even a small error in measurement of the resistance can cause a large error in the measurement of the temperature [8].

1.5THERMOCOUPLE

Thermocouples are the most commonly used temperature measuring device in elevated temperature thermal analysis. The assembly of two different metals joined at their ends to have two junctions in a circuit is called a thermocouple. This phenomenon is known as thermo-electric effect as electricity has been produced from heat. The current thus produced is called thermo-electric current. The thermocouple produces a voltage related to a temperature difference. Thermocouples are a widely used type of temperature sensor for measurement and

can also be used to convert heat into electric power. They are inexpensive and interchangeable, are supplied fitted with standard connectors, and can measure a wide range of temperatures. The main limitation is accuracy: system errors of less than one degree Celsius (C) can be difficult to achieve.

1.5.1 Thermoelectric effect :

A thermoelectric device creates a voltage when there is different temperature on each side. Conversely when a voltage is applied to it, it creates a temperature difference. The thermoelectric effect encompasses three separately identified effects- the Seebeck effect, the Peltier effect and the Thomson effect.

1.5.2 Seebeck effect :

It is a phenomenon of generation of an electric current in a thermocouple by keeping its two junctions at different temperatures. The magnitude and the direction of thermo-emf developed in a thermocouple depends upon the nature of metals forming the thermocouple and the differences in temperature of the two junctions. The seeback effect is reversible i.e. if the hot and the cold junctions are interchanged the direction of thermoelectric current is reversed. In the box given below is shown the Seeback series. The metals/alloys are arranged with respect to the direction of electron flow, when the junction of two dissimilar metal are kept at hot junction. For instance, if a junction of Iron and Copper is kept at hot junction, the direction of electrons will be Copper to Iron.

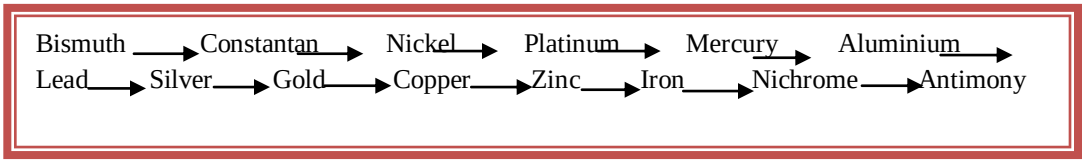

For a given differences of temperature of two junctions the larger is the gap in seeback series between the metals forming the thermocouple, the greater will be the thermo-emf generated. Hence junction of Bismuth/Antimony will generate larger emf than junction of Bismuth/Gold.

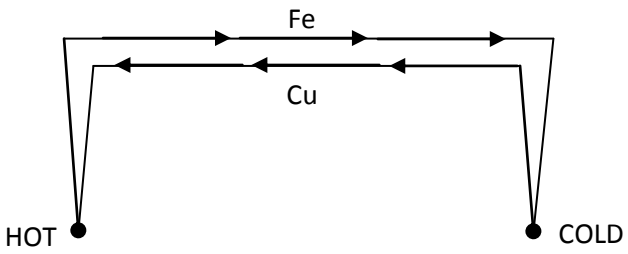

Fig 1.8 : Thermoelectric junction between Iron and Copper for Seeback effect. The arrow denotes the direction of electron flow. The direction of current is opposite to the direction of electron flow

The electron-density (no. of electrons per unit volume) of a conductor depends on the material of the conductor. When two different metals are brought into contact at the junction, the free electrons tends to diffuse from the metal with greater free electron density to the other with lower free electron density. Due to this diffusion, a potential difference developed at the junction of the two metals called contact-potential. When both the junctions are at the same temperature, the contact potentials at the two junctions will be the same. Hence no current flows in the thermocouple. But if one junction is heated up, the rate of diffusion of free electrons at that junction will change, which results in difference in the contact potential of the two junctions called thermo-emf.

$$V_{themo-emf} = V_{hot} - V_{cold}$$

Effect of temperature-When the two junctions of the thermocouple are at the same temperature galvanometer shows no deflection i.e. thermo-emf is zero. If the temperature of the hot junction increases, keeping the cold junction at constant temperature the thermo-emf increases with increase in temperature, until it becomes maximum at certain temperature.

The temperature of hot junction at which the thermo-emf in a thermocouple is maximum is called **neutral temperature (T_n).** When the junction is heated beyond T_n, thermo-emf starts decreasing.

Neutral temperature (T_n) is,

- constant for a thermocouple
- depends upon the material of the material of a thermocouple and
- is independent of temperature of cold junction.

At another particular temperature of hot junction the thermo-emf becomes zero and on further heating, the direction of thermo-emf is reversed. The temperature of the hot junction at which the thermo-emf of the thermocouple becomes zero and just beyond which it reverses its direction is called **temperature of inversion (T_i).**

Temperature of inversion (T_i) depends upon

- the temperature of cold junction and
- on the material of the thermocouple.

$$T_n = \frac{(T_i + T_0)}{2}$$

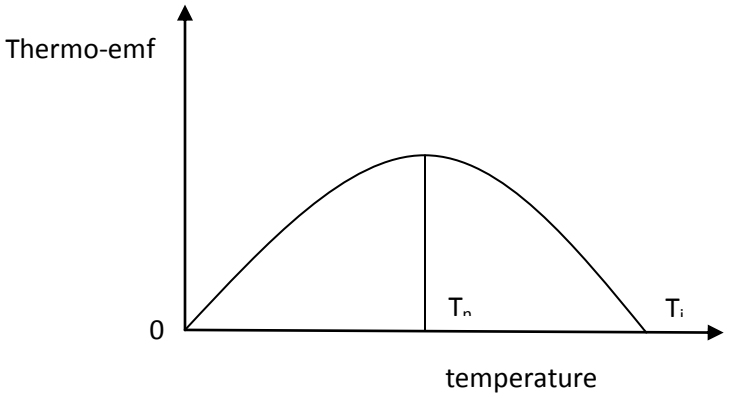

Fig 1.9: Thermo-emf Vs Temperature of a thermocouple.

1.5.3 Peltier Effect :

If a current is passed through a junction of two different metals, the heat is either evolved or absorbed at that junction. This effect is known as Peltier effect. The amount of heat absorbed or evolved at a junction is proportional to the quantity of charge crossing that junction.

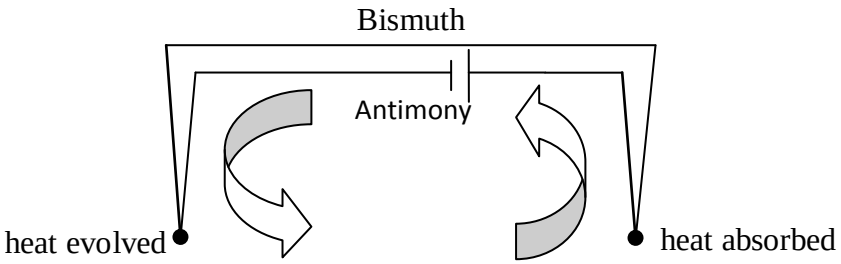

Fig 1.10: Thermoelectric junction for peltier effect

If the direction of current is reversed the heating effect at the junction is also reversed. So, peltier effect is reversible effect. It is also complementary to Seebeck effect. Peltier heat is evolved at a junction of a thermocouple which is kept cold for seebeck effect and the peltier heat is absorbed at a junction of thermocouple which is kept hot for seebeck effect.

Peltier coefficient- Amount of heat energy absorbed or evolved at a junction of two different metals when one coulomb of charge passes through that junction.

$$\Pi = \frac{Peltier\ heat}{Charge\ flowing} \text{ (J/C)}$$

Peltier coefficient depends upon

- nature of the two metals forming the junction and
- Temperature of the junction.

1.5.4 Thomson's Effect :

If two parts of a single conductor are maintained at different temperature, an emf is developed between them. The emf so produced is called Thomson emf. It is the absorption or evolution of heat in excess of joule heat when current is passed through an unequally heated conductor. Thomson effect is reversible effect.

Some substance in which when current flows from hot end to cold end i.e. from higher potential to lower potential, the energy is evolved whereas when current is flowing from cold end to hot end of the rod i.e. from lower potential to higher potential, heat is absorbed , the Thomson effect is positive e.g. Copper, Silver, Zinc, Antimony, etc.

There are some other substances like Iron, Cobalt, Platinum, Bismuth, etc. for which Thomson effect is negative, i.e. heat is absorbed when current is passed from hot to cold end and heat is evolved when current is passed from cold end to hot end of the rod.

In lead (Pb), the Thomson effect is nil i.e. no heat is evolved or absorbed when current is passed through an unequally heated lead.

Thomson coefficient-Amount of heat energy evolved or absorbed between the two points of a conductor maintained at a unit temperature difference when unit current is passed through the conductor.[9]

$$\sigma = \frac{dV}{dT}$$

In a thermocouple,

Seebeck emf = Peltier emf + Thomson emf

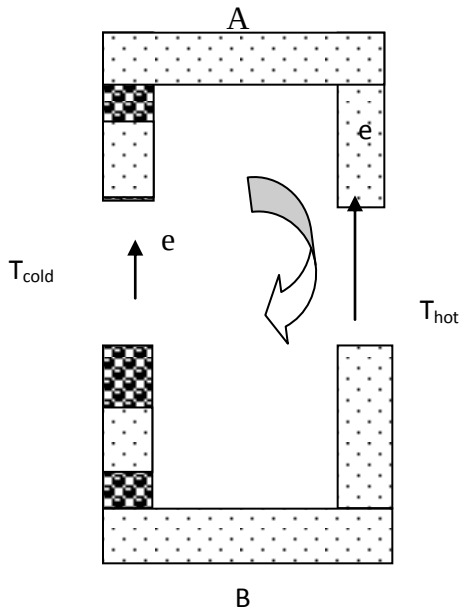

Fig 1.11: free electron model of thermocouple behaviour

1.5.5 Laws of Thermocouple :

- Law of homogenous material- A thermoelectric current cannot be sustained in a circuit of a single homogeneous material by the application of heat alone, regardless of how it might vary in cross section.
- Law of intermediate material- The algebraic sum of the thermoelectric forces in a circuit composed of any number of dissimilar materials is zero if all of the junctions are at a uniform temperature. So If a third metal is inserted in either wire and if the two new junctions are at the same temperature, there will be no net voltage generated by the new metal.
- Law of successive or intermediate temperature- If two dissimilar homogeneous materials produce thermal emf1 when the junctions are at T1 and T2 and produce thermal emf2 when the junctions are at T2 and T3 , the emf generated when the junctions are at T1 and T3 will be emf1 + emf2.[10]

1.5.6 Types of Thermocouples :

Certain combinations of alloy form different types of thermocouples. Selection of the combination is driven by cost, availability, convenience, melting point, chemical properties, stability, and output. Different types are best suited for different applications. They are usually selected based on the temperature range and sensitivity needed.

TYPES	METAL		STANDARD COLOR CODE		IDENTIFICATION		MAX. USEFULL RANGE	
	POSITIVE	NEGATIVE	POSITIVE	NEGATIVE	MAGNETIC LEAD	STIFFEN LEAD	TEMP(^{O}C)	Emf (mV)
B (oxides)	Pt (30% Rh)	Pt (6% Rh)	Grey	Red		+ve	0-1700	0-12.4
E (non-magnetic)	Chromel	Constatan	Violet	Red			-200 to 900	-8.8 to 68.8
J	Iron	Constatan	White	Red	+ve		0-750	0-42.3
N	Nicrosil	Nisil	Orange	Red			-270 to 1300	-4.3 to 47.5
K	Chromel	Allumel	Yellow	Red	-ve		-200 to 1250	-6.0 to 50.6
R	Pt (13% Rh)	Pt	Black	Red		+ve	0-1450	0-16.7
S	Pt (10% Rh)	Pt	Black	Red		+ve	0-1450	0-15.0
T	Cu	Constatan	Blue	Red			-200 to 350	-5.6 to 17.8
C	W (5% Re)	W (26% Re)	White	Red			0-2320	0-38.6

Table 1.3: Types of thermocouple and their properties [9].

1.6 OBJECTIVE

The objectives of the present research are:

1) To design a high temperature resistivity set-up using 4-probe, K-type thermocouple and platinum resistance thermometer (PRT).
2) To prepare a ceramic oxide sample (test sample) for resistivity study.
3) To study the temperature dependent resistivity of the sample prepared.

CHAPTER-2

INSTRUMENTATION

This chapter gives the details of design and fabrication of high temperature resistivity setup which can measure both thin and bulk samples for a temperature range of 300K to 500K. The set up involves a controlled furnace and four probe resistance measuring probe station with temperature control and measurement unit. The task of interfacing of the entire measurement unit (nanovoltmeter, current source) is done with a computer system to enable remote automatic operation and control with minimum manual effort. A preliminary investigation was conducted first to study the temperature stability and ramping control on the power supplied to the designed furnace.

2.1 FURNACE DESIGNING

In order to provide a hot variable temperature to the four probe measuring setup, our first task is to design a furnace which can go to the desirable high temperature. A "wound furnace" was made where a refractory metal wire is wrapped around the alumina tube. For our case Kanthal wire is chosen because it can provide temperature as high as 1000^{o}C. Length of the wire which gives a resistance of 50 ohms is cut and a coil is made from this wire. The coil so made is wound over the alumina tube. In order to keep the winding intact and firm, an insulating adhesive was applied over the winding.

To make the insulating adhesive, ceramic brick (made up of silicon and aluminum) is crushed to fine powder, which is then mixed with sodium silicate gel to make a paste to be used as cementing material. This paste is then applied over and between the gaps of the coil wound over the alumina tube, to avoid overlapping of the coil. Then the tube assembly (kiln) is left for one week for drying.

The outer body of furnace is made from stainless steel container, commercially available in the local market. Before putting the kiln inside the SS container, a thick layer of ceramic wool is put

in the base. On the steel container, three holes are made, one for the control thermocouple which touches the kiln to measure its temperature and two holes for the electrical connection to the coil.

All the holes are well insulated using ceramic beads. The heating coil (Kanthal) wound over the alumina was provided three layers of insulation to get the best temperature stability and minimum heat loss. The first layer is the ceramic brick + sodium silicate pasted and dried over the coil. The second layer is the dry ceramic brick powder tightly packed around the klin. Then the last layer of ceramic wool nicely packed after the ceramic brick powder. The ceramic wool is very light weight and can withstand a temperature up to 1200^{o}C. The use of ceramic wool makes the furnace light weight.

The electrical power to the furnace is given via temperature controller. The working details of the temperature controller are shown in the block diagram below. The temperature of the furnace is sensed via T-type thermocouple connected to the ON/OFF controller. This ON/OFF controller cannot control more that 3 amp of current, hence a automatic electromechanical switch is made using Relays capable of carrying 10-15 amp of current. The output of the ON/OFF controller is fed in a step down (220 to 12V) transformer. This transformer is used to control the relay, connected in series with the AC mains and Furnace. However when the relay is ON, full 220V is applied across the furnace coils, which may heat the furnace to overshoot the set temperature. In order to sweep the temperature very slowly, a potential divider arrangement is added between the relay and the furnace. Using the potential divider arrangement, the current in the coil can be controlled for desired sweeping rate and set temperature. It should be noted that potential divider arrangement is necessary not only to control the sweeping rate, but also to set the temperature to desired values with minimum fluctuation.

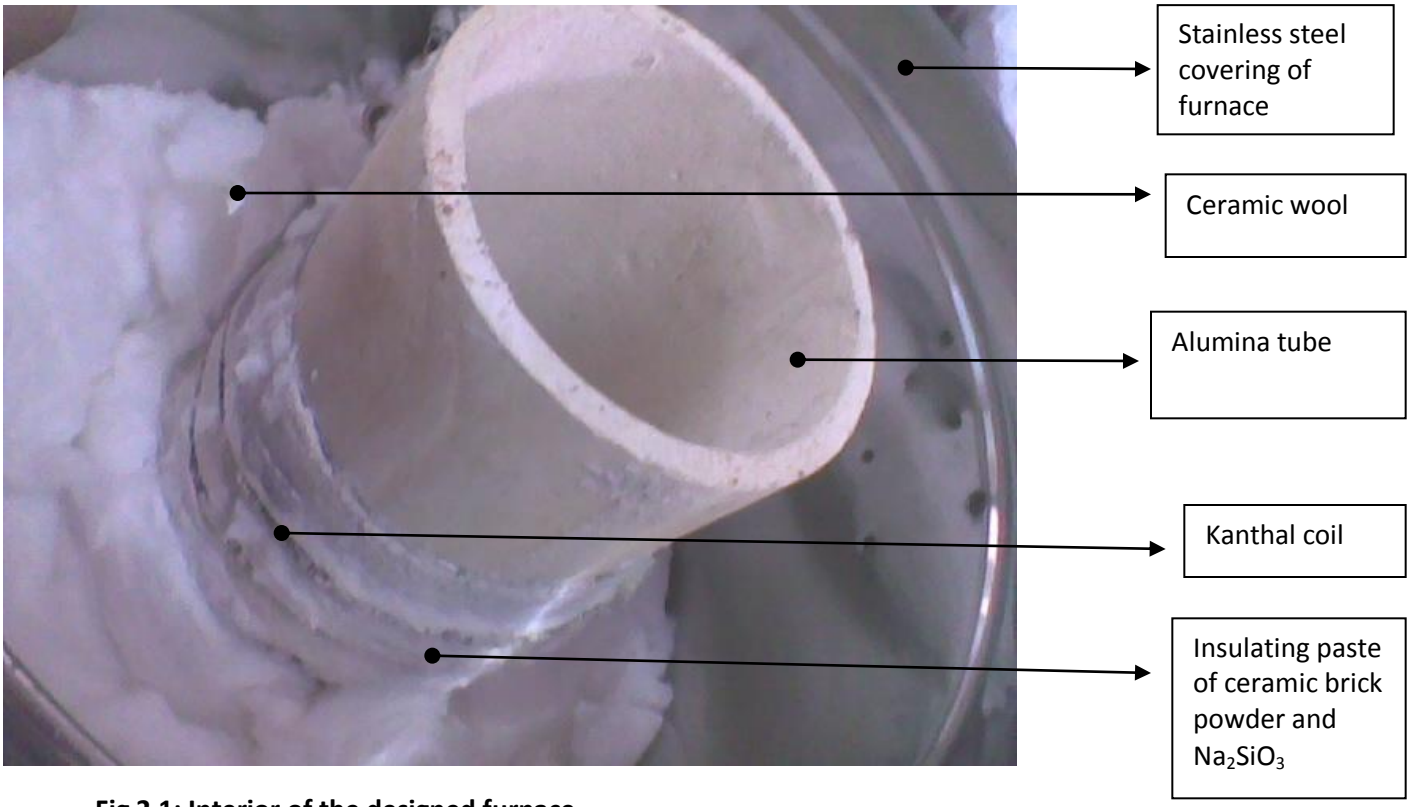

Fig 2.1: Interior of the designed furnace

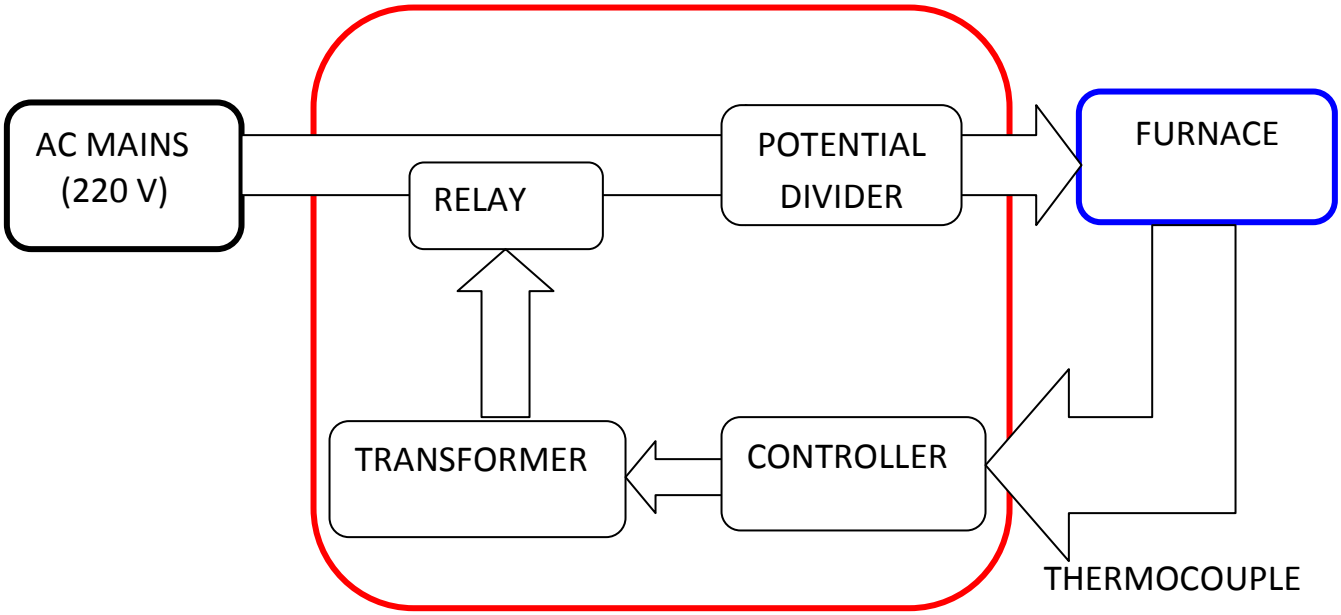

Fig 2.2: Block diagram of ON/OFF furnace control

2.1.1 Automatic control system:

1. **On-Off Control:** Set point temperature is the desired temperature of the furnace at any given time. If the furnace temperature is above the set point, the furnace shut-off. If the furnace temperature is below the set point, the furnace goes to full power. As a result the furnace temperature tends to oscillate about the set point value. As on-off switching fatigues mechanical relay with time, a dead-band is often introduced where by the system does not shut off until the furnace temperature exceed few degree and does not turn on until the furnace temperature drops below the set point by few degrees. The introduction of dead band will increase the amplitude of oscillation but decrease its frequency, preserving the life of the relay.

2. **Proportional Control:** It eliminates furnace temperature oscillation by applying the correction which is proportional to the deviation from the set point.

PID (Proportional Integral Derivative) control system

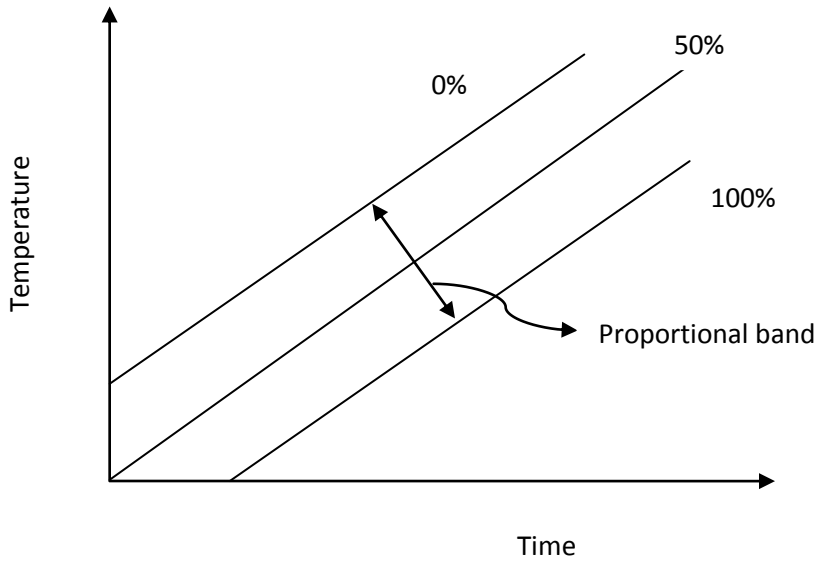

Fig 2.3: Graphical representation of Proportional control system

A proportional band is assigned so that if the furnace temperature exceeds these outer limits, the system reverts back to on-off control.

If the proportional band is adequately broad, the furnace temperature does not oscillate rather it runs parallel to the set point and if the proportional band is too narrow, the furnace temperature will oscillate as if under on-off control. This elimination of parallel ramping is done by an integral function which continuously sums the difference between furnace and set point temperature as swept through the time.

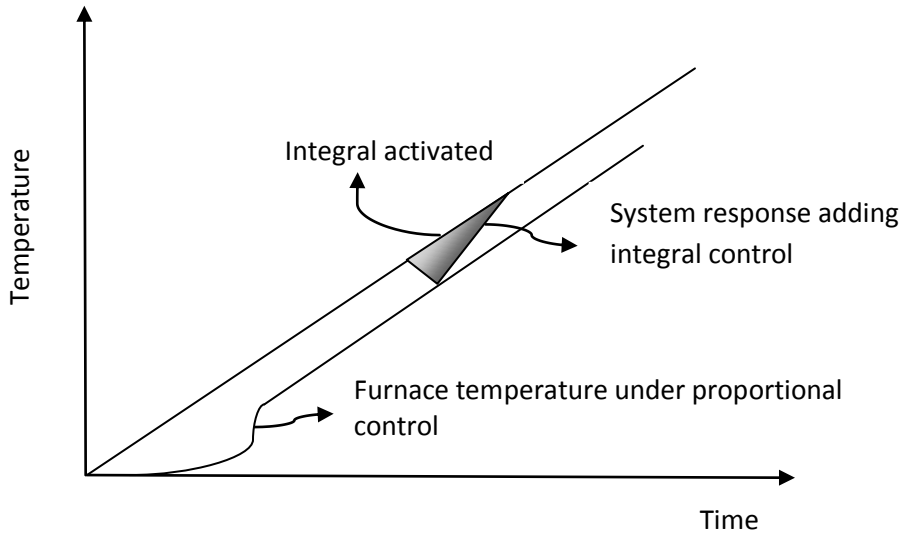

Fig 2.4: Graphical representation of integral control system

This area multiplied by a weighing factor is added to the proportional portion of the control instruction. If the furnace temperature is persistently below the set point, this area continues to accumulate until the furnace temperature is forced up to the set point at which time no additional area is accumulated.

When the furnace temperature lags a desired temperature behind that of set point, the SCR permits more power through and eventually the furnace temperature rise with so much momentum that it overshoots the set point. To minimize overshooting and undershooting effects derivative control may be introduced.

The derivative function strives to keep the slope of the furnace temperature with time the same as that of set point with time.

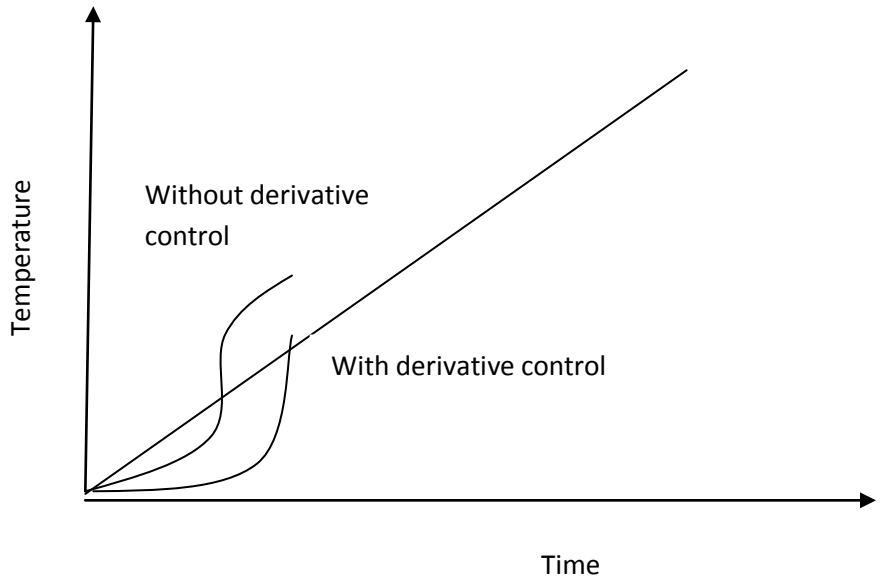

Fig 2.5: Graphical representation of derivative control system

Derivative control acts as a predictive function, whereby if the temperature is below the set point, but is rising rapidly, it (multiplied by a weighing constant) subtracts power from the control instruction. So that it coincides with set point minimizing overshoot.[11]

PID control system is represented as

$$P = P_0 - U_P(T - T_S) - U_I \int_0^t (T - T_S)dt - U_D(dT/dt - dT_S/dt)$$

Where P=power

P_0=arbitrarily assigned starting power

T=furnace temperature

T_S=set-point temperature

U_P, U_I and U_D are proportionality constant for proportional, integral and derivative respectively.

In the designed system, an on-off temperature controller was used for high temperature measurement. The temperature controller was then calibrated with the increase in the percentage of power supply by every 10 degree rise in temperature from 100^0 C to 500^0 C. The figure below shows the calibrated graph of the furnace temperature controller.

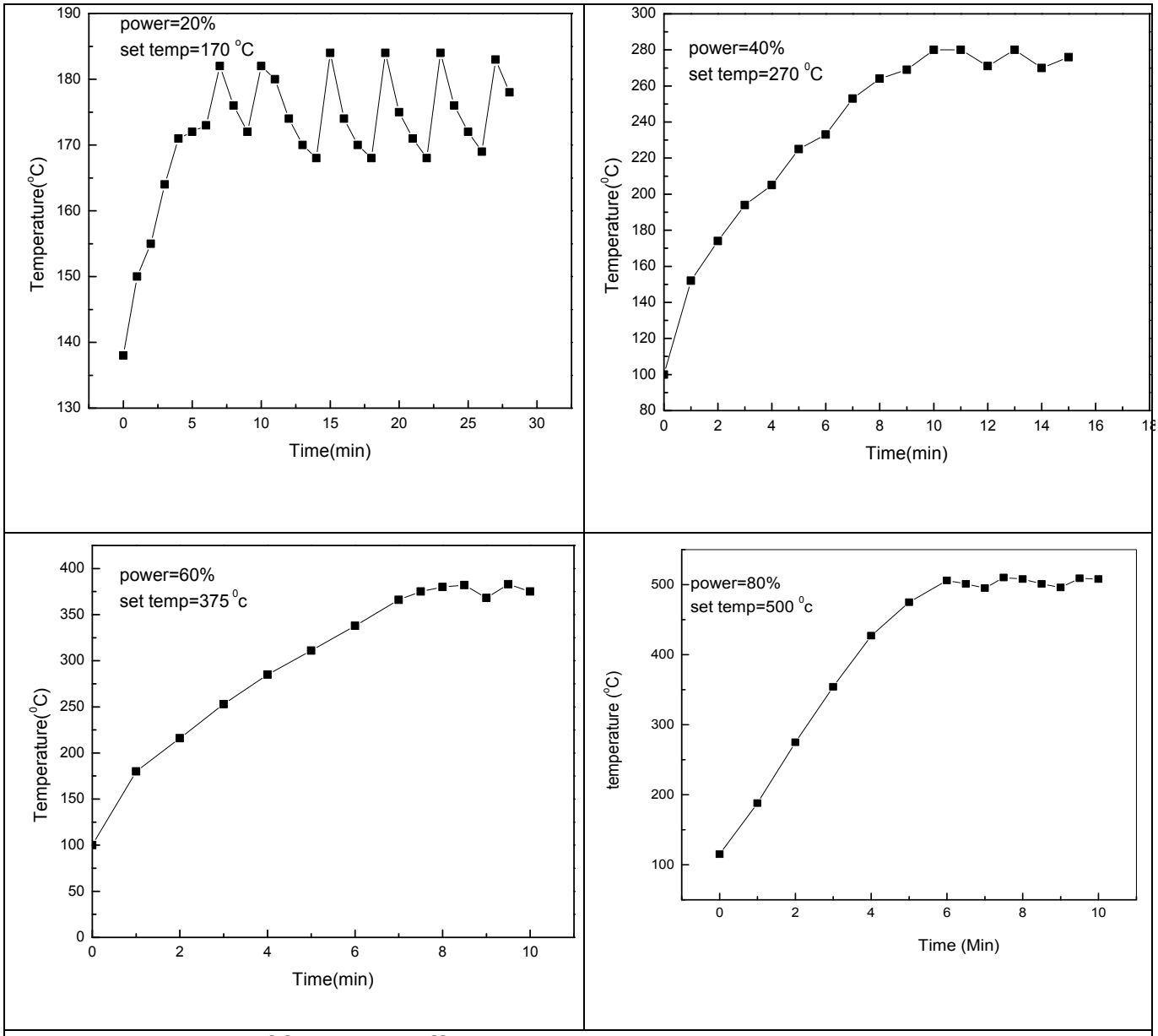

Fig 2.6: Calibration of furnace at different power and set temperature

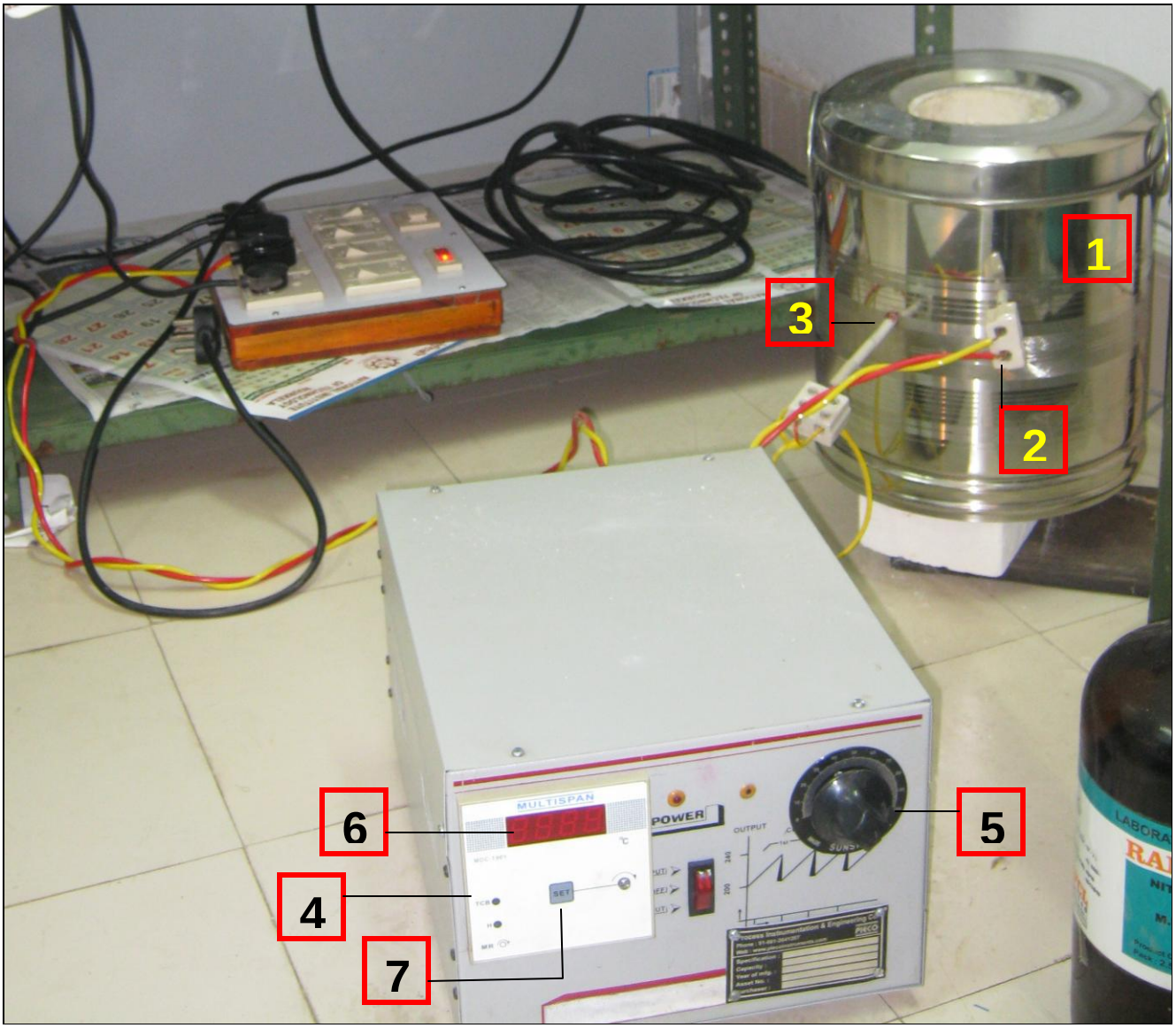

Fig 2.7: Furnace with temperature controller [1] Furnace; [2] Porcelain connectors for electrical connection; [3] thermocouple; [4] Temperature controller; [5] Power regulator; [6] Digital panel; [7] Set point adjust

2.2 FOUR PROBE ASSEMBLY

The actual working four probe setup is shown in the fig 2.8. The assembly is supported on three SS studs. Two copper disks of width 8mm and diameter 8cm is cut from a solid cylindrical copper rod. Copper is chosen for this purpose, because of good thermal conductivity to the sample. An aluminium sheet of dimension 11 x 11 cm was cut from a large sheet. Three 4mm holes are drilled over all the three metal plates in a tripod like manner so that studs can be inserted which act as a supporting stand. In one of the copper disk (middle) and aluminium sheet, a hole of 8.2mm was drilled at the center so that ceramic beads containing four copper wires can be inserted. Near the central hole, another hole of 6.5mm was drilled to insert Pt-100 sensor, resting over the bottom copper base. In the aluminium plate 8.5mm hole was drilled in the same line as in the copper disk where 6.5mm hole is placed. The three metal plates are assembled together at a distance of 6.5cm from each other with the help of three studs and nuts. Four equal sized copper wires of length 23cm was cut and sharpened at the ends. These four copper wires were insulated by inserting them inside four–holed ceramic beads. This assembly is inserted in the central hole of the four probe system.

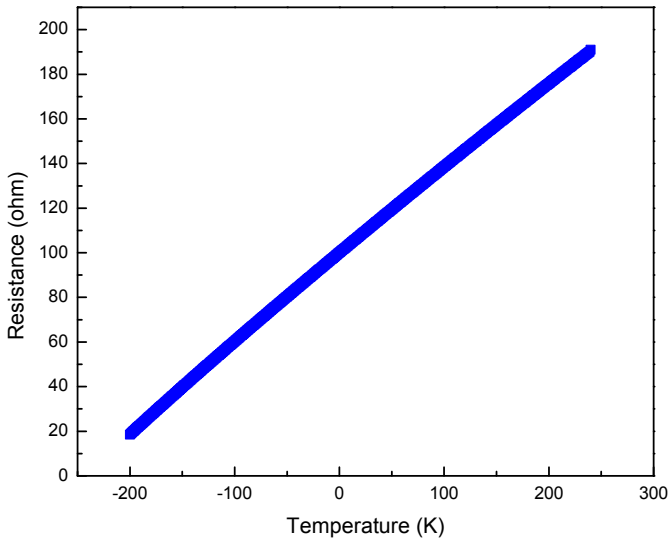

Fig 2.8: Resistance vs. temperature plot of the used Pt-100 sensor [12]

Out of the four copper wires of the four probe, two are connected to Keithley nanovoltmeter for voltage measurement and other two were connected to Keithley current source which supplies constant dc current to the probes. Pt-100 sensor is connected to a digital ohmmeter for the measurement of resistance with the variation of temperature. Keithley nanovoltmeter and Keithley current source was interfaced with the computer using Labview software for the resistance measurement.

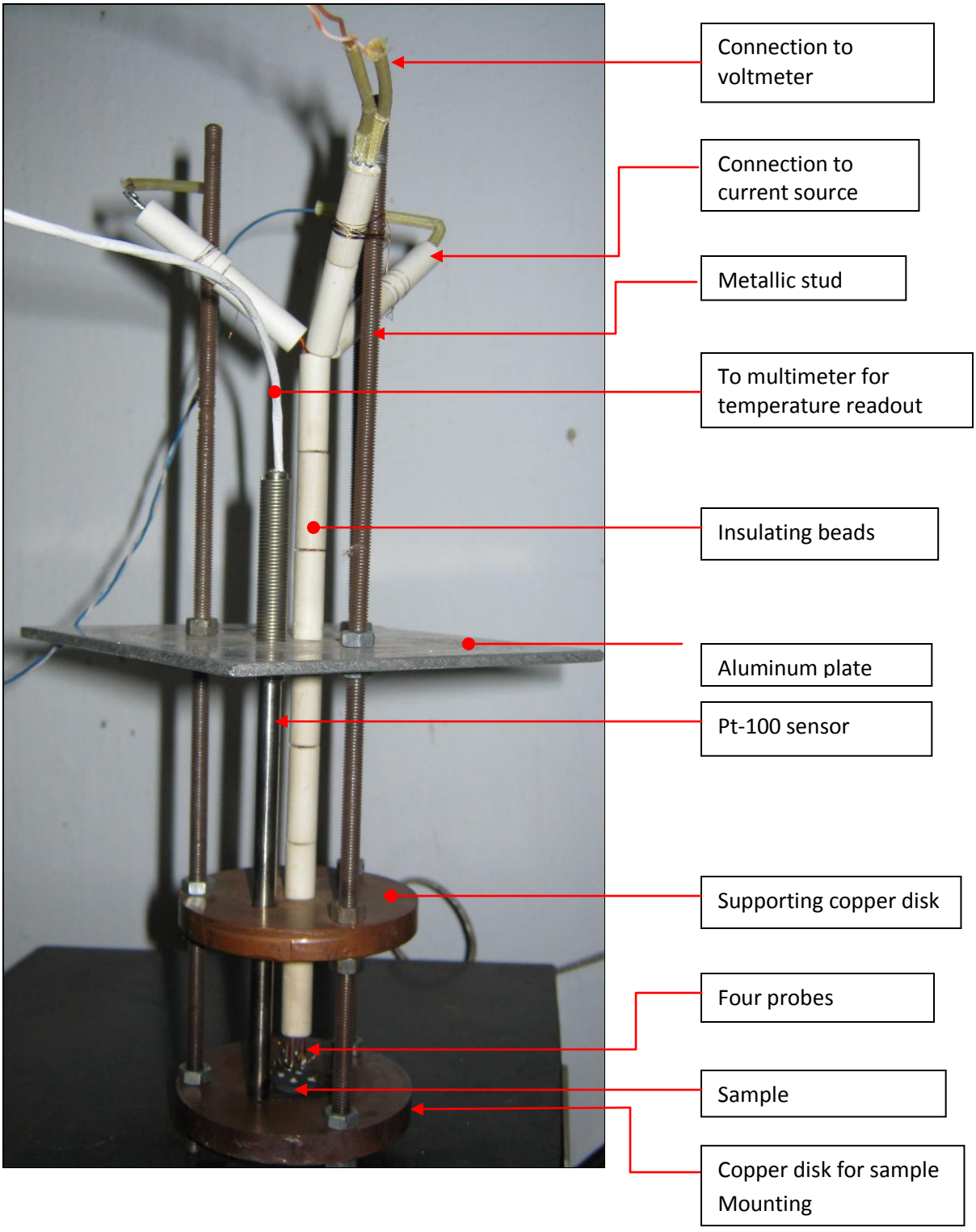

Fig 2.9: Four probe assembly

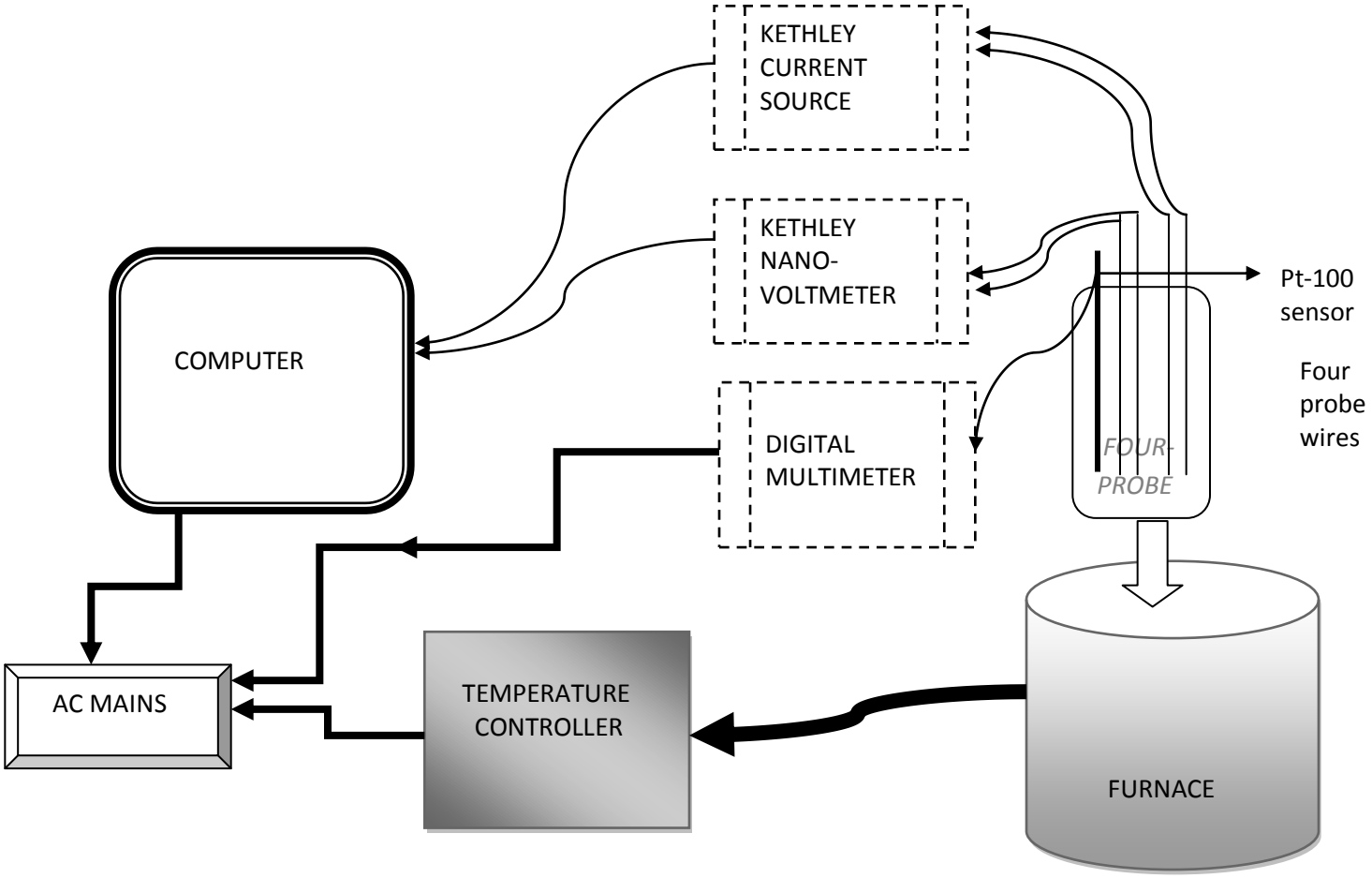

Fig 2.10: Block diagram for the designed high temperature resistivity measurement set-up

CHAPTER-3

SAMPLE PREPARATION

3.1 CHOICE OF SAMPLE

Lanthanum manganite ($LaMnO_3$) is an anti ferromagnetic insulator which when doped with strontium; undergo metal-insulator transition and Ferro-paramagnetic transitions at T_c and T_P respectively. Lanthanum strontium manganite is an oxide ceramic material with general formula $La_{1-x}Sr_xMnO_3$, where x describes percentage of doping of strontium. It has pervoskite structure which is generally of the form ABO_3 with Lanthanum and strontium occupying the corner of the crystal (A type cations), manganese occupy the body centre position of the crystal (B type cations) and oxygen occupies the face centre position of the crystal (O type anions).[13]

3.2 PROPERTIES OF LSMO

LSMO are half metals with manganese configuration Mn^{+3}, while Mn^{+4} gave rise to metallic state with negligible spin polarization at the Fermi level. The electronic property of LSMO is described by band theory that reflects the so called transport half-metallic behavior. By changing doping concentration, electrical and magnetic properties can be tuned. For x = 0.3, it has almost 100% spin polarization and high Curie temperature (T_c=360 K). It has large magnetic moment at room temperature [14].

3.3 APPLICATIONS OF LSMO

1) The half-metallic nature of LSMO is used in spintronic devices. So it can be used in microelectronics. The technology of spintronics required the electron spin to carry the information. So the devices have an extraordinary property which arises from the interaction between the spin of the carrier and the magnetic properties of the material. The devices thus formed are smaller, denser and can store information which can store information which can be processed by manipulating the spin of electrons [15].

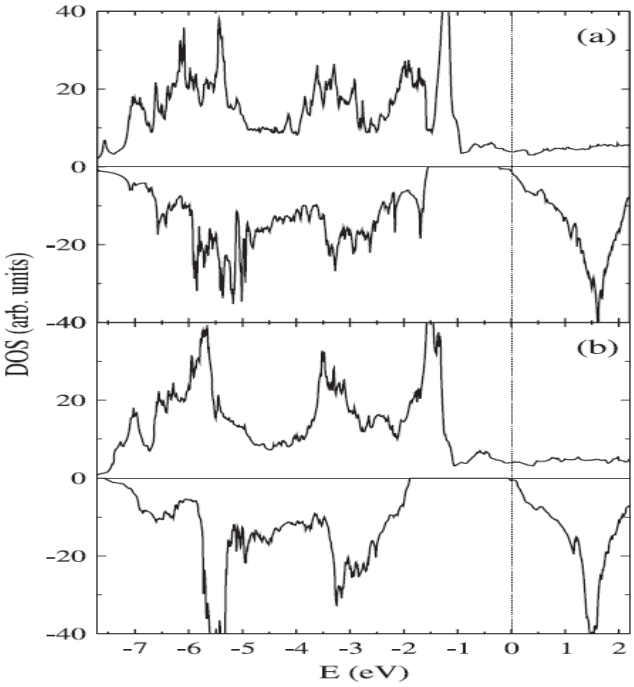

Fig 3.1: Spin resolved density of states of LSMO [16]

At the Fermi level (shown by dotted line) only up-spin electrons are present and down spin are negligible. So only half of the spin is contributing and thus is called half-metallic [17].

2) The colossal magnetoresistance is another property of LSMO which can be used in magnetic sensors. It can be defined as the change in the electrical resistance produced by the application of an external magnetic field. There is a change in behavior of resistivity with temperature. So the system is metallic below T_c and insulator activated in the paramagnetic region [15].

3) In hyperthermia application, magnetic nanoparticles of fairly uniform size, having curie temperature above room temperature are required. Due to high T_c value (about 360K) and a large magnetic moment at room temperature, LSMO is a best material to use [18]. It has a large applicability in biomedicine because there is no change in curie temperature at 360 K after conjugation with biomolecules, rapid attachment of desired temperature (48^oC) at low concentration upon exposure to 20 MHz radio frequency, extremely low cytotoxicity in skin carcinoma, human fibrosarcoma and neuroblastoma cell lines and

stability of LSMO system with negligible leaching of ionic manganese into delivery system [19].

4) It is used as cathode of solid oxide fuel cells (SOFCs) due to its high electrical conductivity at high temperature and the thermal expansion match with yittria-stabilised zirconia(YSZ) which is SOFCs electrolytes [20].

5) LSMO motors and geared motors used in machine tools in wet environment to ensure reliable operation in oil and drilling industries [21].

6) The figure 3.2 shows the temperature dependence of resistivity of LSMO. No ferromagnetic phase transition is observed for concentration $x \leq 0.05$. It shows a non-metallic behavior for $x \leq 0.2$. With the increase in 'x' it shows a metallic behavior with the shifting of T_c towards high temperature [22].

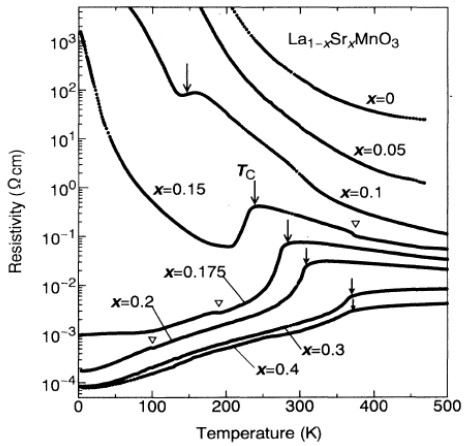

Fig 3.2 : Temperature dependence of resistivity for LSMO crystal [22]

7) Below the magnetic transition temperature, three phase are present spin-canted anti ferromagnetic insulator (CNI) in low doped region ($x < 0.1$), a ferromagnetic insulator (FI) in the region 0.1 to 0.15 and a ferromagnetic metal (FM) in high doped region $x > 0.15$. Above the magnetic transition temperature (T_c and T_N) the non-metal to metal transition takes place at x=0.3 [22].

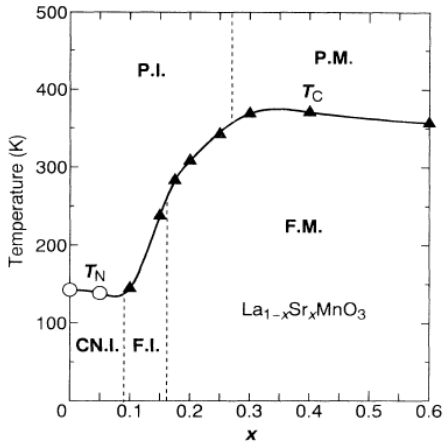

Fig 3.3: Electronic phase diagram of LSMO[22]

3.4 LSMO PREPARATION

Some of the conventional methods of LSMO preparations are,

- ✓ Sol-gel soft chemical method[23]
- ✓ Solid-state method[24]
- ✓ Pulsed laser deposition method[25]
- ✓ Metalorganic deposition technique[26]
- ✓ Carbonate precipitation route[27]
- ✓ Floating zone method[28]
- ✓ Spray dryer method[24]

The components corresponding to the formula $La_{0.66}Sr_{0.33}MnO_3$ is prepared by sol-gel method. The precursors used are Manganese carbonate ($MnCO_3$), Lanthanum nitrate $(LaNO_3)_3$, Strontium nitrate $(Sr(NO_3)_2)$ and the fuel used is glycine. At first a starting solution of nitrate precursors are separately made by mixing $MnCO_3$ (20 mmol) with minimum amount of concentrated nitric acid (HNO_3) and $La(NO_3)_3$ (66% of 20 mmol) and $Sr(NO_3)_2$ (33% of 20 mmol) in distilled water. All these solutions are mixed and to this resultant solution glycine is added in stochiometric proportion (metal:glycine= 1:1). The solution is stirred and slowly evaporated over hot plate at ~ 100^oC in order to form the gel which then burnt to form black powder. This obtained powder is then grinded for 2 hrs. This grinded powder is then pressed into pellet and then sintered at 820 ^0C for 5 hrs. The obtained sample is then characterized through XRD.

Flow chart:

Fig 3.4: Flowchart for LSMO preparation

RESULTS AND DISCUSSION

4.1 SAMPLE CHARACTERIZATION

4.1.1 X-ray diffraction analysis:

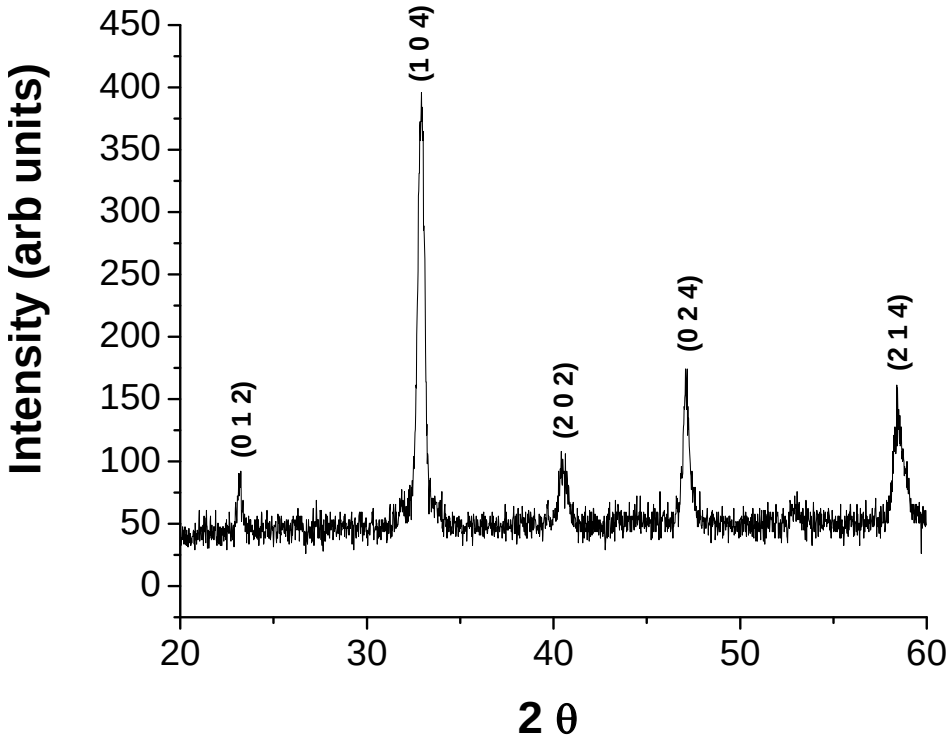

Fig 4.1 X-ray diffraction pattern of LSMO

Figure 4.1 shows the room temperature XRD pattern of LSMO. The sharp and well defined single diffraction peaks, which are different from those of the precursors, confirm the formation of single phase of LSMO. The observed XRD pattern matched with the standard XRD pattern of LSMO (ICDD-401100). The peak position (2θ), full width at half maximum (FWHM), and intensity of each peak are calculated using a commercially available software (PEAK FIT) [29]. Indexing of XRD patterns is carried out using diffraction angle (2θ) and intensity value of each peak by least-squares method with the help of software (POWDMULT) [30]. The best agreement

between the observed interplanar-spacing and Bragg angles with the calculated one, results the orthorhombic crystal structure. The least squared refined lattice parameters are found to be a=3.855(2) A^0, b=3.837(2) A^0 and c=3.880(2) A^0 and the unit cell volume is 57.38(2) $(A^0)^3$ (the standard deviations are in parenthesis).

4.1.2 Williamson-Hall method:

The broadening of X-ray diffraction peaks is mainly due to crystallite size and strain of the material. The Williamson-Hall method was used to find out the crystallite size and rms value of strain of LSMO sample using the following equation:

$$\beta\cos\theta = 4\varepsilon\sin\theta + \frac{\lambda}{D}$$

where, β is the FWHM of XRD peaks , D is crystallite size and ε is the rms strain respectively. By plotting βcosθ vs. 4sinθ, strain can be calculated from the slope and crystallite size can be calculated from the ordinate intercept.

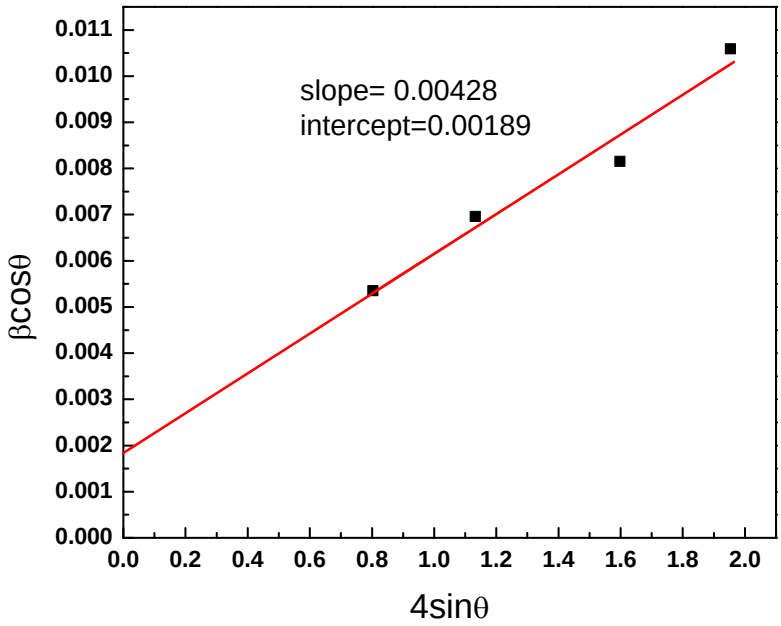

Fig.4.2 Williamson Hall plot of LSMO.

The Williamson–Hall plot of LSMO is shown in figure 4.2. From the graph, D is found to be 81.5 nm and strain is found to be 0.00428.

4.2 RESISTIVITY MEASUREMENT

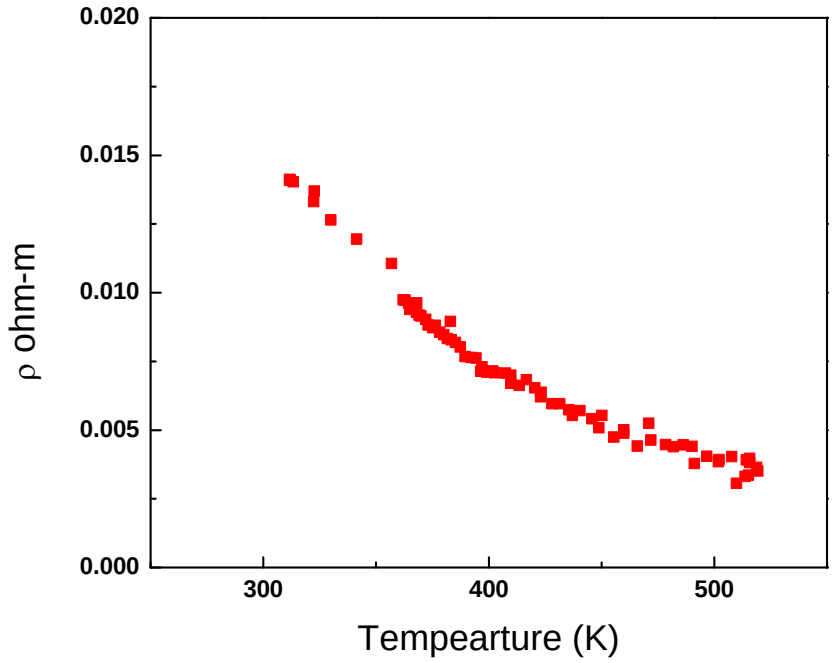

Fig 4.3 Resistivity Vs. Temperature graph of LSMO.

Figure 4.3 shows the resistivity vs. temperature graph of LSMO. The resistivity of the LSMO sample is measured by four probe set up using Keithley nano-voltmeter 2182 and Keithley current source 6221. The measurement is carried out in a temperature range of 300K to 500K in a self-made furnace. Electrical contacts to the sample are made via conducting silver epoxy, in accordance with the Van-der Pauw method. A constant current is applied to two consecutive probes and the voltages at different temperatures are measured at the other two probes. All the data except, Pt100 resistance are collected in a PC via Lab View programming. The values of Pt100 resistance is noted down manually, as the multimeter had no option of interfacing. From the obtained resistances, resistivity can be calculated as

$$\rho = \pi R d / \ln 2$$

where, ρ is the resistivity, R is the measured resistance, and d is the sample thickness. The resistivity of LSMO decreases with the increase in temperature.

4.2.1 Calculation of activation Energy:

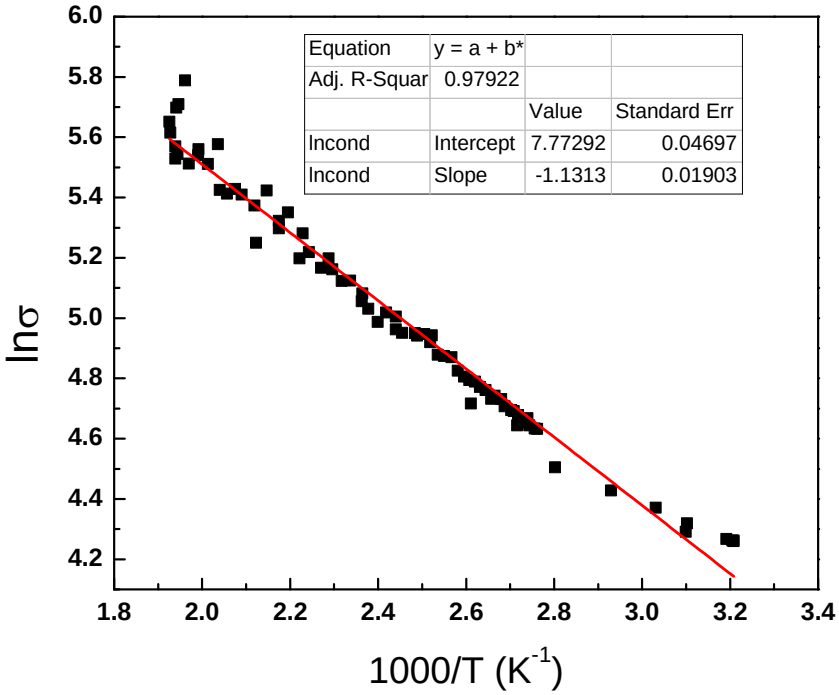

Fig 4.4 Arrhenius plot of resisitivty data for LSMO.

The variation of dc conductivity with the inverse of temperature is shows in figure 4.4. It is observed that the curve follows the Arrhenius equation,

$$\sigma_{dc} = \sigma_0 \times \exp\left(-E_a / k_B T\right) \Rightarrow \ln \sigma_{dc} = \ln \sigma_0 - \frac{E_a}{k_B T}$$

where, σ_0 is the pre-exponential factor, E_a is the activation energy, k_B is the Boltzmann constant and T is the temperature in kelvin. By plotting, $\ln(\sigma_{dc})$ vs.1000/T ,we can calculate activation energy (E_a) from the slope of the graph. The solid line is the straight line fit used to obtain the slope. Activation energy of a sample is the energy that must be overcome in order for a electrical conduction to occur i.e. the minimum energy required to start electrical conduction. The activation energy calculated from the slope is found out to be 0.09758 eV.

CHAPTER-5

CONCLUSION AND FUTURE SCOPE OF RESEARCH

5.1 CONCLUSION

A furnace which can withstand about 600^0C temperature was successfully developed which involves a four probe assembly, sample holder, temperature control and measurement unit. The designed furnace was calibrated at different power percentage and the graph at higher temperature was found to be almost linear with time. The synthesis of LSMO sample was done by sol-gel method. XRD analysis confirms the formation of this magnetite structure. The dc resistivity of LSMO was studied extensively.

Based on results, the following conclusion can be drawn.

- From the XRD analysis, it was found that LSMO has orthorhombic structure.
- The temperature vs. resistivity graph suggests that LSMO is half metallic.
- The lattice parameters were calculated using standard software POWD and it was found to be a= 3.8550 A^0, b= 3.8367 A^0 and c= 3.8794 A^0.
- Williamson hall method was used to determine crystallite size and strain which was found to be 81.52 nm and 0.00428 respectively.
- Activation energy was calculated using Arrhenius equation and was found to be 0.09758 eV.

5.2 FUTURE WORK

- We have measured the resistivity of the sample from room temperature (30^0C) to 280^0C by heating and cooling. For better analysis of electrical properties, resistivity below room temperature can be studied using liquid nitrogen as cooling agent.

- At higher temperature due to thermal expansion of the copper wires used in four probes, we do not show accurate result. To avoid this pressure contacts can be made on the wires of the four probes that touches the sample surface perfectly throughout the experiment.
- Our setup has only provision for measuring resistivity of a given sample. The set up can be bettered by designing it to measure simultaneously many electrical properties of a material such as dielectric constant, activation energy along with resistivity.

APPENDIX

This is a collaborative project which is done with my pew mate, Kalyani Bhoi. We have made two ceramic oxide samples (LSMO and cobalt ferrite). Both the samples are prepared through sol-gel soft chemical method. The XRD characterisation of both the samples are done simultaneously. The details of the cobalt ferrite sample preparation and characterisation can be find out from the thesis of Kalyani Bhoi. Some of the results are summarised below,

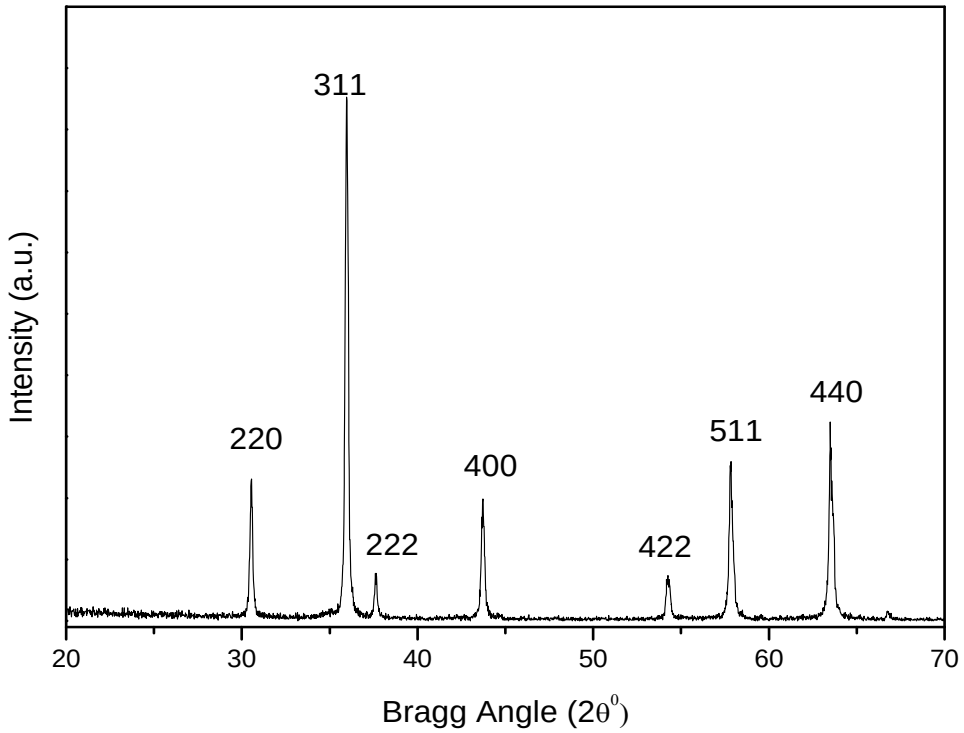

Fig 1: X-ray diffraction pattern of CFO

The crystal structure is found to be cubic with lattice parameter a=8.391 (49) A^0 and the unit cell volume is 84.58 (49) $(A^0)^3$ (the standard deviations are in parenthesis).

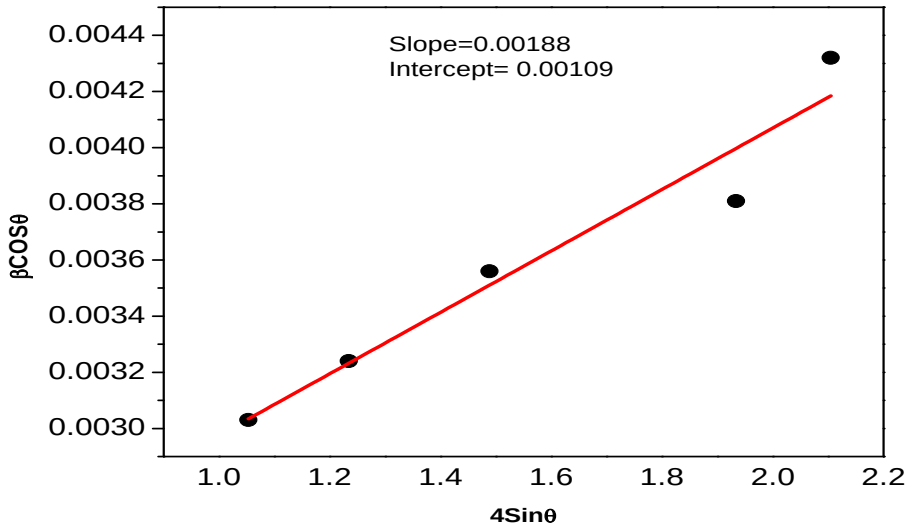

Fig. 2: Williamson Hall plot of CFO.

From the Williamson Hall plot of cabalt ferrite the crystallite size is found to be 141.35 nm and strain to be 0.00188.

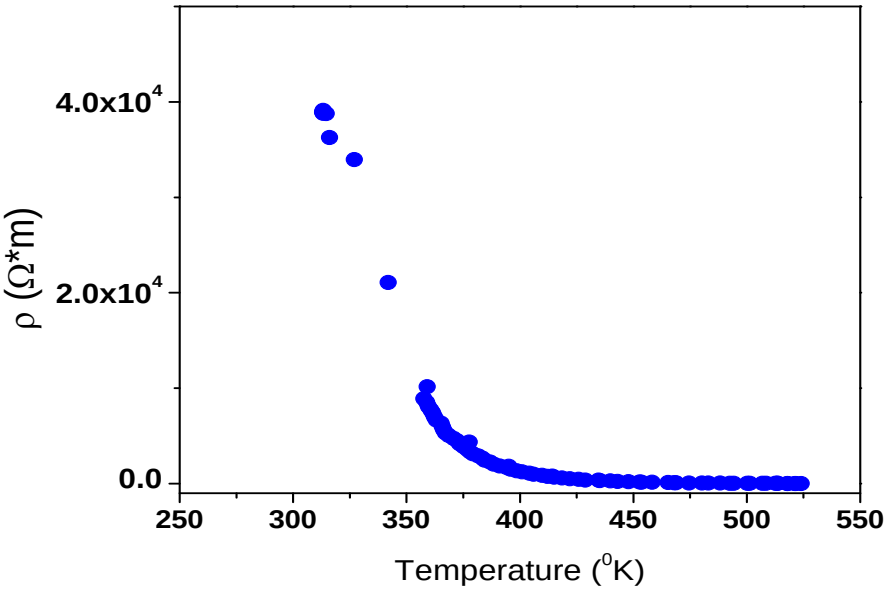

Fig.3: Temperature dependent resistivity of CFO.

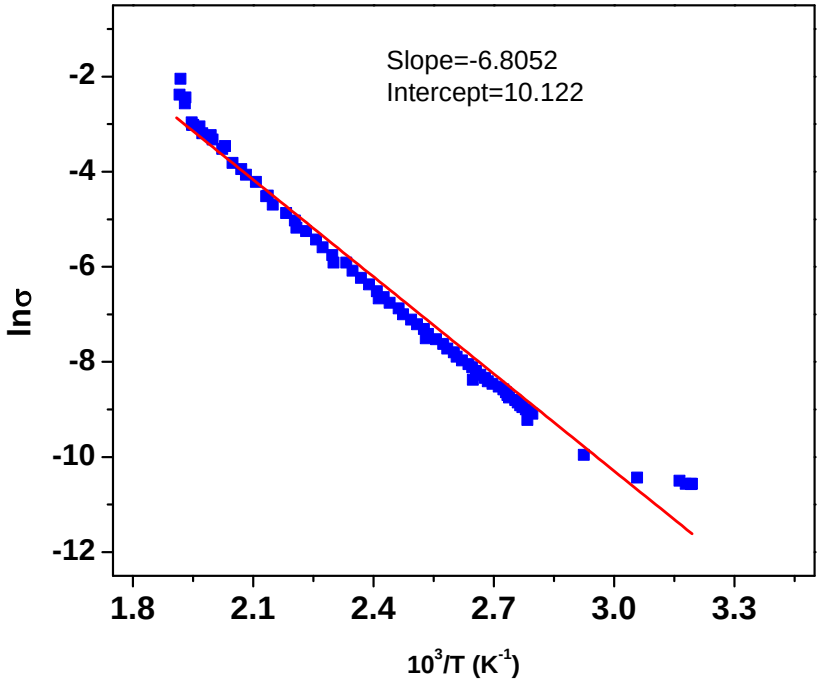

Fig.4: Variation of σ_{dc} with inverse of temperature of CFO.

The activation energy calculated from the slope is found out to be 0.586 eV.

REFERENCES

[1] Resistance www.wikipedia.com

[2] www.teachers.web.cern.ch

[3] www.earthsci.unimelb.edu.au

[4] www.spiff.rit.edu

[5] www.omega.com

[6] www.omega.com/temperature/z/pdf/z033-035.pdf

[7] www.maitreyi.du.ac.in

[8] www.picotech.com/applications/pt100.html

[9] K.L Gomber and K.L Gogia, Fundamental of Physics.

[10] Thermocouple www.wikipedia.com

[11] Robert F.Speyer, Thermal analysis of materials.

[12] www.intech.co.nz/product/temperature/typert.html

[13] LSMO www.wikipedia.com

[14] G.Banach et.al, Study of half- metallicity of LSMO, Elsevier Science.

[15] Juraj Krempasky, Angle and spin-resolved photoemission on La2/3Sr1/3MnO3, University of Ce4gy- Pontoise.

[16] B.Zheng and N. Binggeli, Effects of chemical order and atomic relaxation on the electronic and magnetic properties of La2/3Sr1/3MnO3, J. Phys: condens. Matter 21 (2009) 115602.

[17] Warren E.Pickett and David Singh, Electronic structure and half- metallic transport in the La1-xCaxMnO3 system, Physical review, volume-53, Number-3, 1996.

[18] Ali Rostamnejadi et.al, Particle size effect on magnetic properties of interacting La0.67Sr0.33MnO3 nanoparticles, Isfahan University of Technology, 84156-83111, Iran.

[19] Sangeeta N.Kule et.al, Ceramic doping and stochiometry ncontrol for biomedical use of La0.7Sr0.3MnO3 nanoparticles, Science direct, volume-2, issue-4,2006, pages 217-221.

[20] LSMO www.wikipedia.com

[21] www.leroy-somer.com/documentation-pdf/depliants/3800a-en.pdf

[22] A.Urushibara et.al, Insulator- metal transition and giant magnetoresistance in La1-xSrxMnO3, Physical review B, volume-51,number-20, 1995.

[23] Javier Bermejo et.al, Spin relaxation in nanophased manganites, Journal of Non-crystalline solids 354 (2008) 5258-5260.

[24] D.Grossin and J.G.Noudem, Synthesis of fine La0.8Sr0.2MnO3 powder by different ways, Elsevier Science, 6 (2004) 939-944.

[25] J.M.Liu et.al, Oxygen deficiency activated anamolous transport in La2/3Sr1/3MnO3 thin films deposited by Laser ablation, J.Phys: condens. Matter 14 (2002) 3167-3173.

[26] Donald T.Morelli et.al, Magnetocaloric properties of dopped Lanthanum Manganite films, American Institute of Physics 1996 (S0021-8979(96)09101-7).

[27] M.Pekala et.al, Magnetocaloric and magnetic materials, volume-322, issue-21, 2010, pages 3460-3463.

[28] L.Pinsard et.al, Structural phase diagram of La1-xSrxMnO3 for low Sr dopping, Journal of Alloys and compounds, 262-263 (1997)152-156.

[29] Jandel scientific software, version-4 for win32, AISN software Inc.(1991-1995).

[30] Jandel scientific software, version-4.02, 1991.